Springer

Acta Mechanica Sinica

CrossMark click for updates

• REVIEW •

Acta Mech. Sin., Vol. 39, 323019 (2023)
https://doi.org/10.1007/s10409-023-23019-x

On modelling fluid/body interactions, impacts and lift-offs

Frank T Smith[1*], Ellen M Jolley[1], and Ryan A Palmer[2,3]

[1] *Department of Mathematics, University College London, London, UK;*
[2] *School of Biological Sciences, University of Bristol, Bristol, England;*
[3] *School of Mathematics, University of Bristol, Bristol, England*

Received January 13, 2023; accepted February 3, 2023; published online March 24, 2023

A description is given of recent progress in the understanding of mechanisms in fluid-body interactions where the motion of a body and the motion of the surrounding fluid affect each other substantially. The mathematical modelling of such unsteady interactions is for internal channel and external near-wall flows in two spatial dimensions and time. The emphasis throughout is on analytical developments with accompanying reduced computation. The successive aspects studied here are interactions and impacts in inviscid flows, skimming and sinking, the lift-off, fly-away or bouncing of a body, and viscous effects including especially the interplay between viscous and inviscid contributions. The main findings are concerned with physical and mechanical insights into impact times, lift-off criteria, the borders between impact and fly-away, the principal parameters and their ranges and the influences from body shape and mass.

Fluid-body interactions, Skimming, Impacts, Analysis

Citation: F. T Smith, E. M Jolley, and R. A Palmer, On modelling fluid/body interactions, impacts and lift-offs, Acta Mech. Sin. **39**, 323019 (2023), https://doi.org/10.1007/s10409-023-23019-x

1. Introduction

This contribution is essentially a review on recent progress in the understanding of dynamic fluid-body interactions. A dynamic fluid-body interaction involves the unsteady motion of a solid body (particle, object) that is freely moving in a surrounding fluid and affecting the fluid flow substantially, which thereby affects the body motion substantially and produces two-way interplay.

The scenarios of practical and scientific concern have an incident unidirectional or almost unidirectional fluid flow over a solid wall but with a free finite two-dimensional or three-dimensional body located initially above the wall such that part of the oncoming fluid travels through the gap between the underneath of the body and the wall. This yields an unsteady two- or three-dimensional interaction. The concern in this contribution will be almost entirely with the two-dimensional case as a basis for increasing understanding. Moreover, the solid wall mentioned above may be the lower wall of a channel or it may be situated in an external flow; both setups will be considered in the review.

The focus in the present article is specifically on analytical developments that are described in the stream of papers [1-22]. These are mostly on interactions arising in two spatial dimensions (say x, y) and time t. A very recent development is in Ref. [23] which is concerned with three spatial dimensions (thus x, y, z, t). The above studies examine two-dimensional (2D) dynamic fluid-body interactions in boundary layers of nonzero shear flow, e.g., Refs. [7, 14-16, 20, 21], in uniform near-wall flow, e.g., Refs. [4, 11, 22] and in channel flows, e.g., Refs. [1, 6, 11], with the typical flow rates of interest being high in relative terms: in other words the representative Reynolds number is large. The flow pressure on the body surfaces then provides the major force from the fluid dynamics and this acts to continuously move (accelerate or decelerate) the body and rotate it, therefore altering the fluid dynamics itself and so continuing the two-way interplay.

*Corresponding author. E-mail address: f.smith@ucl.ac.uk (Frank T Smith)
Executive Editor: Shizhao Wang

In the background are the main motivations which concern practical applications for example to: the safety of land, sea and air vehicles when impacted upon by ice particles, droplets or debris; the travel of objects, drugs or thrombi in human arteries and lungs; the motion of dust, dirt and sand on Earth and other planets; and the travel of grains such as rice down chutes in food-sorting machines. This is in addition to the scientific and technological curiosity and challenge of the subject. Also in the background are many other interesting papers most of which are on direct numerical simulations and experiments within the large area of fluid-body interactions. These address boundary layers [24-29], channel flows [30, 31] and include predictions for flow transition [24-26, 28, 31] and turbulent motion [27, 29, 30]. There are also analyses on flow at relatively low flow rates.

Our prime concern is with phenomena occurring at high Reynolds numbers and involving dynamic fluid-body interactions for thin or slender fluid layers and bodies. The phenomena to be considered are either, on the one hand, for inviscid or quasi-inviscid fluids or, on the other, for viscous-inviscid configurations. The work to be described uses mathematical modelling on a rational basis typically leading to reduced systems of equations; this is coupled with analysis for example in the form of matched asymptotic expansions to account for the effects of high Reynolds number, slender bodies and upstream or downstream influence, and allied with numerical studies whenever necessary and experimental or observational findings wherever possible. The work here also concentrates on properties for a single thin body although the original study [1] allowed for many bodies in an aligned formation, while a very recent extension [32] is to two or more bodies in a non-aligned setup. Channel flow, boundary layer flow, skimming, sinking, lift-off, rebounds and combined viscous and inviscid effects are to be described.

The plan of the paper is as follows. Section 2 presents the fundamental interactive reasoning and equations of interest. Section 3 then addresses inviscid fluid-body interaction in channel flows and in external flows, including descriptions of various types of impact between the body and the wall or boundary. Skimming and sinking are considered in Sect. 4, while features of lift-off, fly-away and bouncing are considered in Sect. 5. Section 6 describes the influences of viscous effects with specific interest in viscous-inviscid interplay and flow separation, followed by Sect. 7 which provides further discussion and conclusion.

2. Modelling and formulation

In view of the background and motivations described in the introduction, we model here a dynamic fluid/body interaction for a single body of uniform density $\rho_{\rm DB}$, mass $M_{\rm D}$ and moment of inertia $I_{\rm D}$ in the presence of an oncoming flow of fluid of density $\rho_{\rm DF}$ with typical velocity $u_{\rm D}$ in the $x_{\rm D}$ horizontal direction. We let $y_{\rm D}$ measure distances in the vertical direction. See Fig. 1. The fluid is assumed to be incompressible and its flow to be laminar, the body is rigid but free to move, and spatially the fluid/body interaction is 2D. The working herein is with Cartesian coordinates $(x_{\rm D}, y_{\rm D}) = L_{\rm D}(x, \epsilon y)$, corresponding velocity components $u_{\rm D}(u, \epsilon v)$, pressure $\rho_{\rm DF}u_{\rm D}^2 p$ and time $L_{\rm D}u_{\rm D}^{-1}t$, where $L_{\rm D}$ is for example the typical length of the body in the horizontal direction while ϵ denotes the typical ratio "vertical (lateral) distance"/"horizontal (streamwise) distance", or angle, of the interaction and of the body's vertical and horizontal dimensions.

Our eventual interest is mostly in small ϵ, associated with thin or slender bodies in thin-layer flows. If however ϵ is treated as being of order unity then the non-dimensional Navier-Stokes equations apply

$$\frac{\partial \mathbf{u}}{\partial t} + (\mathbf{u}\cdot\nabla)\mathbf{u} = -\nabla p + Re^{-1}\nabla^2\mathbf{u}, \tag{1}$$

coupled with the continuity equation $\nabla\cdot\mathbf{u} = u_x + v_y = 0$. Here $Re = u_{\rm D}L_{\rm D}/\nu_{\rm D}$ is the Reynolds number where $\nu_{\rm D}$ is the kinematic viscosity of the fluid. In many applications Re is large and so subsets of Eq. (1) become important. One is the Euler system in which the diffusion effect becomes negligible, leaving the inviscid form:

$$\frac{\partial \mathbf{u}}{\partial t} + (\mathbf{u}\cdot\nabla)\mathbf{u} = -\nabla p, \tag{2}$$

provided the flow is separation-free. A third system is that of the boundary layer equations which hold for small ϵ, formally when $\epsilon = Re^{-1/2}$, giving the horizontal momentum

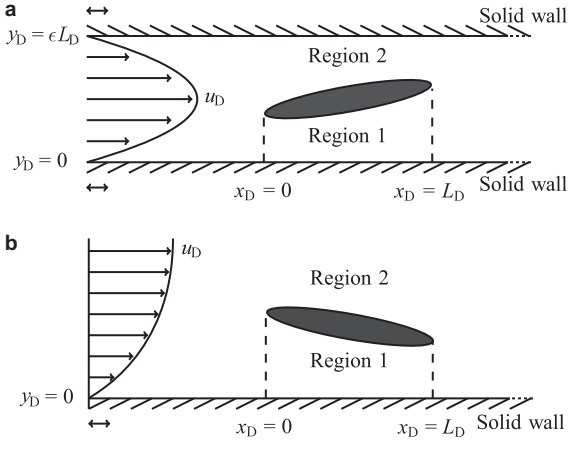

Figure 1 Interaction between fluid flow and a freely moving body **a** in a channel, **b** in external flow, sketched (not to scale) with the body travelling upstream or downstream relative to the wall(s). The typical flow velocity is $u_{\rm D}$ and the body length is $L_{\rm D}$.

balance:

$$u_t + uu_x + vu_y = -p_x(x,t) + u_{yy}, \tag{3}$$

whereas the y-momentum balance establishes that the pressure $p(x,t)$ must be independent of y. The fourth system of interest is the inviscid version, in which

$$u_t + uu_x + vu_y = -p_x(x,t), \tag{4}$$

again for values of ϵ that are small. Equations (1)-(4) describe the fluid-flow contributions to the overall interaction or in some cases describe subsets of the flow, for example near the leading edge of a body. Throughout, the continuity equation remains as stated earlier.

Complementing the above equations of fluid flow are the body-motion equations based on Newton's laws of motion, specifically the product of mass and acceleration must balance the relevant forces acting on a body. If $(x, \epsilon y) = (X_c, Y_c)(t)$ denotes the moving centre of mass of the body and $\theta_c(t)$ its angle of rotation then in general:

$$M\frac{\mathrm{d}^2X_c}{\mathrm{d}t^2} = F_x, \quad M\frac{\mathrm{d}^2Y_c}{\mathrm{d}t^2} = F_y, \quad I\frac{\mathrm{d}^2\theta_c}{\mathrm{d}t^2} = N,$$

where F_x and F_y are the integrated forces produced by the fluid motion supplemented by gravity and N is the integrated torque or moment. Here M and I denote the non-dimensionalised mass and moment of inertia respectively. When ϵ is small these body-motion equations of linear and angular momentum simplify in view of the smallness of $\theta_c(t)$, yielding the leading-order relations:

$$\frac{\mathrm{d}^2X_c}{\mathrm{d}t^2} = 0, \tag{5a}$$

$$M\frac{\mathrm{d}^2h}{\mathrm{d}t^2} = \int_0^1 (p_1(x,t) - p_2(x,t))\,\mathrm{d}x \; - \; M\hat{g}, \tag{5b}$$

$$I\frac{\mathrm{d}^2\theta}{\mathrm{d}t^2} = \int_0^1 (x-C)(p_1(x,t) - p_2(x,t))\,\mathrm{d}x, \tag{5c}$$

with $\theta_c(t) = \epsilon\theta(t)$, $Y_c = \epsilon h(t)$. The relation (5a), which stems from the property that the integrated horizontal force is comparatively small, implies that $X_c = At + C$ where A and C are constants but in addition the coordinate frame taken is fixed horizontally with that of the body, thus leading to $A = 0$ as well as making the integration ranges in Eqs. (5b) and (5c) be $(0,1)$ and leaving the centre of mass at $x = C$ where $0 < C < 1$. The pressure forces acting on the body surfaces as in Fig. 1 are the major contributions from the fluid flow, with p_1, p_2 representing in turn the pressures on the lower and upper surfaces of the body.

The boundary and initial conditions on the interactive system also play a very significant role which is described in the following sections.

3. Inviscid model: interactions and impacts

Here we consider internal flow past a free body within straight channel walls in Sect. 3.1 below followed by external flows in Sect. 3.2. The study includes impacts onto a solid wall. Account is taken of the possible largeness of the body density ρ_{DB} relative to the fluid density ρ_{DF} especially when the fluid is air for example.

3.1 Impacts in channel flows

The channel-flow scenario [1)] [1,3,11] is considered in some detail below: see also Fig. 1a. It concerns just a single body, together with the parameter ϵ being small and the pressures p_1, p_2 being comparable. Equation (4) holds in the two thin regions above and below the body.

The specific configuration addressed here has a uniform oncoming flow $u = u_0(y) = 1$ (plug flow) in the channel at $x = 0^-$. The boundary conditions on the system (4) are to ensure tangential flow at the channel walls, impose the kinematic conditions at the body surfaces, set a Bernoulli requirement across the Euler zone at the leading edge of the body and set a Kutta condition at the trailing edge. Thus the conditions are, respectively,

$$v = 0 \text{ at the walls } y = 0, 1, \tag{6a}$$

$$v = f_t + uf_x \text{ at } y = f(x,t), \text{ with } f = f_1 \text{ (lower surface)}$$

$$\text{and } f = f_2 \text{ (upper)}, \tag{6b}$$

$$p + \frac{1}{2}u^2 = \frac{1}{2} \text{ at } x = 0^+, \tag{6c}$$

$$p = 0 \text{ at } x = 1. \tag{6d}$$

The moving surfaces of the body are given by

$$f(x,t) = F(x) + h(t) + (x-C)\theta(t), \tag{7}$$

with $F(x) = F_1(x)$ and $F = F_2(x)$ denoting the given fixed shapes of the underbody and overbody respectively in the absence of motion. As a result of the incident plug flow and the quasi-steady nature of the Euler zone where x is small and $O(\epsilon)$ the conservation property (6c) holds. Additionally the vorticity is zero virtually everywhere to leading order and so it follows that $u = u(x,t)$ is independent of y. Hence the kinematic requirement (6b) combined with the tangential requirement (6a) leads to the relation:

$$H_t + (Hu)_x = 0, \tag{8a}$$

1) Q. Liu, Interactions, Impacts and Rebounds of Fluid and Body Motions in Channels, Dissertation for Doctoral Degree, UCL (University College London), in preparation.

where the gap widths H are given by $H = H_1 = f_1(x,t)$ in the lower thin layer and $H = H_2 = 1 - f_2(x,t)$ in the upper layer; meanwhile Eq. (4) reduces to the form:

$$u_t + uu_x = -p_x. \tag{8b}$$

Equations (8a)-(8b), which are the so-called shallow water equations, hold in each of the thin layers below and above the moving body. A final constraint is that of conservation of total mass flux, requiring

$$u_1 H_1 + u_2 H_2 = 1 \text{ at } x = 1. \tag{9}$$

This is inferred from an integral of Eq. (8a). The initial state of the system typically has h, h', θ, θ' prescribed together with initial values $u(x,0)$. The fluid-body interaction is completed by the linkage with the body-movement equations (5b)-(5c).

The above formulation includes the localised upstream influence due to the Euler zone which is generated close to the leading edge. In the zone Eq. (2) applies but with the unsteady terms being negligible because of the shortened x scale locally and hence the Bernoulli conservation law (6c) is obtained, as discussed. There is no further upstream influence ahead of the Euler zone in the present small-ϵ model.

An instability analysis is of interest here. Given that an exact solution of the interaction system for the case of an aligned flat plate in the middle of the channel has uniform flow with zero pressure variation, we consider small perturbations of the form:

$$(H,u,p) = \left(\frac{1}{2},1,0\right) + \delta\left(H^{(1)},u^{(1)},p^{(1)}\right) + \ldots, \tag{10}$$

with δ small. Substitution into Eqs. (8a)-(8b) leaves at leading order the linearised equations:

$$H_t^{(1)} + H_x^{(1)} + u_x^{(1)} = 0, \tag{11a}$$

$$u_t^{(1)} + u_x^{(1)} = -p_x^{(1)}, \tag{11b}$$

subject to boundary conditions derived from linearization of Eqs. (5b), (5c), (6c), (6d), and (9). When body thickness is negligible the time-dependence can be shown to be exponential, proportional to $\exp(Qt)$ say, with the eigenvalue constant Q to be found. The eigenvalue equation obtained is

$$(3M+1)\left(I+\frac{1}{180}\right)Q^3 + \left(3MI + \frac{M}{10} + 4I + \frac{1}{20}\right)Q^2 - \left(\frac{M}{2} - 6I - \frac{1}{5}\right)Q + \left(\frac{1}{3} - M\right) = 0, \tag{12}$$

in addition to the presence of two zero-Q roots which are associated with uniform translation. The left-hand side of Eq. (12) establishes that for any $M > 1/3$ there is a single eigenvalue with a positive real part. Eigenvalues are plotted in Fig. 2. The fact that the typical eigenvalue is $O(1)$ indicates the modelled interaction exhibits instability but only over the time scale of the complete interaction, not over shorter or longer time scales.

A typical computational solution of the nonlinear system is presented in Fig. 3, showing the temporal evolution of the leading- and trailing-edge heights $y_{\rm LE}, y_{\rm TE}$ respectively given by $h - C\theta$, $h + (1-C)\theta$. This is for a flat-plate body with centre of mass at the midpoint. Comparisons [1] between previous computational results and the prediction (12) prove affirmative for low-amplitude behaviour. At higher amplitudes an impact (a crash or clash) between the body and one of the walls, as indicated in Fig. 3, is a possible outcome.

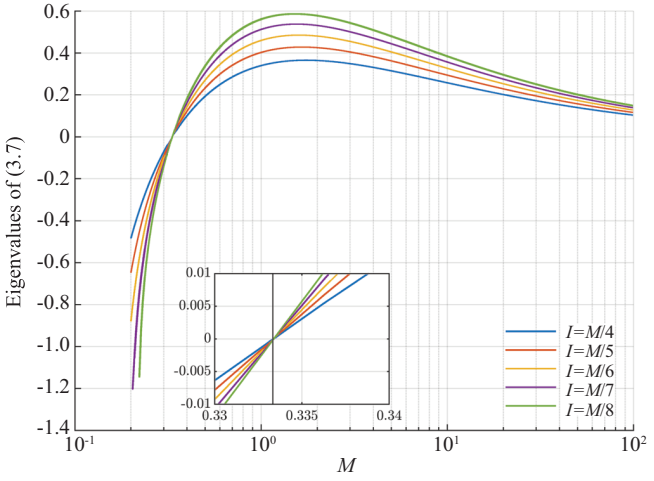

Figure 2 Plots of the eigenvalues given by Eq. (12) versus M for several I values.

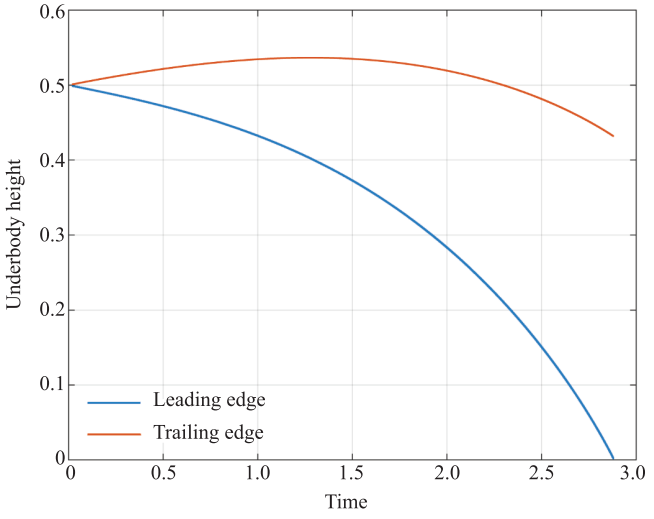

Figure 3 A sample solution for the full system (6a)-(9) coupled with Eqs. (5b) and (5c) in a channel. The body is a flat plate with $F(x)$ zero, $C = 1/2$, $(M,I) = (2, 0.4)$, initial $(h, h', \theta, \theta') = (0.5, 0, 0, -0.1)$; shown are the leading- and trailing-edge heights as functions of time t.

Concerning such impacts, an impact at a sharp leading edge of a body is investigated analytically by Ref. [1], occurring at a finite time $t = t_0^-$, say. It is shown that the expansion:

$$h(t) = h_{10} + (t_0 - t)h_{11} + \delta(t)h_{12} + \dots, \tag{13a}$$

where h_{10}, $h_{11}, \dots$ are constants and the scale factor δ is given by

$$\delta(t) = (t_0 - t)/\ln(t_0 - t) + \dots, \tag{13b}$$

describes an impact on the lower wall, with an expansion for $\theta(t)$ similar to that in Eq. (13a) but such that $\theta_{10} = 2h_{10}$ because of closure of the lower gap at the leading edge. The sensitive logarithmic dependence present in Eqs. (13a) and (13b) is notable.

On the other hand, impact at a mid-body position is addressed in Ref. [3] for a smooth non-flat surface: here the expansion takes the form:

$$h(t) = h_{10} + (t_0 - t)h_{11} + (t_0 - t)^{3/2}h_{12} + \dots, \tag{14a}$$

with a similar expression holding for $\theta(t)$. Locally near the impact position $x = x_0$ at $t = t_0$ the fluid velocity and pressure assume the forms:

$$u = (t_0 - t)^{-\frac{1}{2}}U_1(\xi) + \dots, \tag{14b}$$

$$p = (t_0 - t)^{-1}P_1(\xi) + \dots, \tag{14c}$$

where $\xi = (x - x_0)/(t_0 - t)^{\frac{1}{2}}$ is $O(1)$. A non-local expansion both upstream and downstream of the impact position is also significant here, yielding

$$u = O(1) + O\left[(t_0 - t)^{\frac{1}{2}}\right], \tag{14d}$$

$$p = O\left[(t_0 - t)^{-\frac{1}{2}}\right], \tag{14e}$$

subject to matching with the solution of Eqs. (14b) and (14c). The body motion then points to a subtle balance involving the lift and moment due to the pressures active in both the local and the non-local areas.

3.2 Impacts in external flows

The study of impacts in external flows as in Fig. 1b constitutes more recent work [21, 22]. It is similar to the work which has been described above but it accommodates three extra or novel factors. These are: an allowance for the incident flow profile $u_0(y)$ being non-uniform, such as for interaction taking place within an oncoming boundary layer; the property that the mass and moment of inertia values M and I are often large for many realistic bodies; and the feature that whereas the underbody pressure p_1 is typically of order unity the overbody pressure variation p_2 is small because of the necessary match with the external flow outside the boundary layer.

Here there is body-air-wall interaction in which the body travels through an air boundary layer on top of a wall [2] [21]. In some detail we have the following. The governing equations are Eq. (4) coupled with Eqs. (5b) and (5c) but with p_2 neglected, and similarly the boundary conditions remain as in Eqs. (6a), (6b), (6d), and (7) provided the upper surface, overbody effect and upper wall conditions are omitted, while Eq. (6c) is to be described shortly. Only the flow $u = u_1$, $v = v_1$, $p = p_1$ in the gap between the underbody and the wall interacts with the body motion since the flow above the body is given by $u_2 = 1$, $v_2 = p_2 = 0$ in essence. Also taking into account the typical large size of M and I leads to a time scale such that the operator $\partial/\partial t$ becomes negligible in the fluid dynamics, leaving the gap equations:

$$u_x + v_y = 0, \tag{15a}$$

$$uu_x + vu_y = -p_x, \tag{15b}$$

combined with Eqs. (5b) and (5c). Finally here, for a general incident profile $u_0(y)$ the relation (6c) between pre-Euler and post-Euler flows has to be replaced by

$$\begin{aligned}\frac{1}{2}u_0(Y(0^-))^2 &= \frac{1}{2}u(0^+, Y(0^+), t)^2 + p(0^+, t)\\ &= \frac{1}{2}u(x, Y(x), t)^2 + p(x, t),\end{aligned} \tag{16}$$

on a streamline $Y = Y(x)$ say.

A sample solution for a smooth convex underbody is presented in Fig. 4 and it indicates that a "crash" can take place at a finite time $t = t_0^-$. The crash or impact is centred on some position $x = x_0$ with $0 < x_0 < 1$. The behaviour as t tends to t_0^- takes the following form. Near $x = x_0$ we have the h-expansion:

$$h(t) = h_{10} + (t_0 - t)^{4/5}h_{12} + \dots, \tag{17}$$

together with a similar expansion for θ and for the gap width where $x - x_0$ is of order $(t_0 - t)^{2/5}$ locally. This is supplemented by a non-local response which holds for $x - x_0$ values of order unity, i.e., for the remainder of the domain of interest.

A subsequent stage then arises over a shortened time scale during which the $\partial/\partial t$ operator comes back into play significantly in the fluid flow, thus reinstating the governing equation (4). This yields the eventual final impact of the body onto the wall being essentially the same as that found in Eqs. (14a)-(14e) [3]. Discussion of the existence of other outcomes apart from the above impacts is deferred to Sect. 5 below.

2) E. Jolley, Fluid-Body Interactions, Dissertation for Doctoral Degree, UCL (University College London), in preparation.

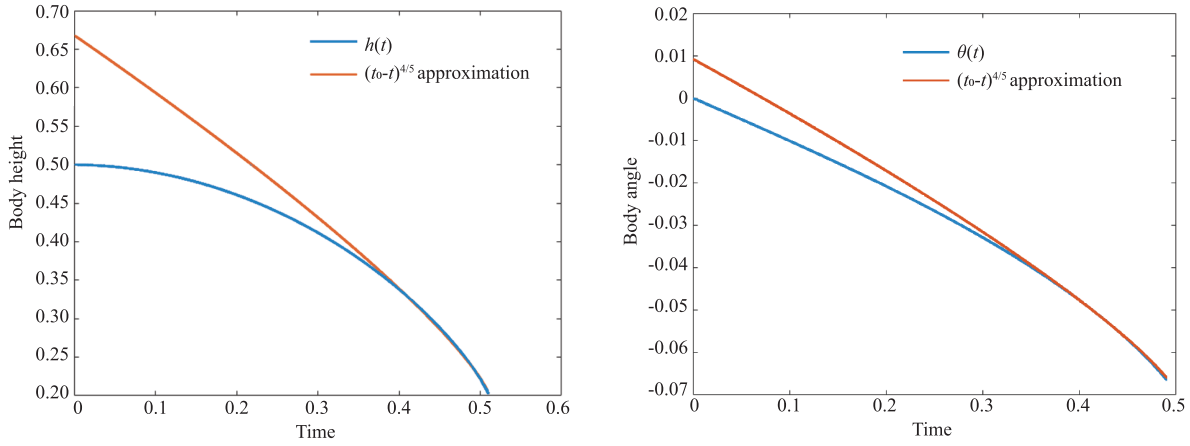

Figure 4 A solution for the reduced system where Eqs. (15a), (15b), and (16) apply.

We should remark in addition that ongoing work developing from the above studies includes investigations of external flow with air motion over a water layer on top of a solid wall. The extra feature of a water layer leads to body-air-water-wall interaction [3]. The latter aspect also brings us to the next section which is concerned with skimming work and related phenomena.

4. Skimming and sinking

The typical skimming of a body in practice occurs when a thin body enters water obliquely, with all the angles involved in the liquid flow, the body and the motion of the body being small. Air may be trapped in this impact process, similar to air cushioning, but usually a mathematical model of skimming treats the air as a void having negligible dynamic influence on the water-body interaction. See Fig. 5 for a defining sketch.

The approach of Ref. [2] which treats air as a void is taken here. The model holds for shallow water and is in essence the same as in the general approach of Sect. 2 with, however, the upper pressure p_2 set to zero (atmospheric) and the underbody pressure p_1 likewise zero except in regions that are wetted or pressurized. The extent of the wetted region varies with time. Thus if the trailing edge of the body enters the water first then the downstream edge of the wetted region is fixed at $x = 1$ whereas the leading edge or moving contact point of the wetted region is at an unknown location $x = x_1(t)$ where $-1 < x_1(t) < 1$ during the skim. Upstream of the contact point the liquid flow has velocity u and height H both identically equal to unity, being undisturbed at leading order. The leading edge of the body itself is fixed at $x = -1$; if $x_1(t) + 1$ ever becomes zero or negative then flooding takes place over the top surface of the body and this can lead eventually to sinking.

The governing equation (4) applies in the water but under certain assumptions of slenderness a linearization also holds which leads effectively to a reduced system akin to that of Eqs. (11a) and (11b). The body-motion equations (5b) and (5c) with zero p_2 and negligible gravity effects act to couple the liquid and body motions together fully, albeit with the range of integration being

$$(x_1(t), 1) \text{ instead of } (0, 1). \tag{18}$$

This is in view of the moving contact point and the wetted region. The boundary conditions of concern apply in the wetted region, namely

$$p = 0 \text{ at } x = 1, \tag{19}$$

$$p + (1 - x_1'(t))u = 0 \text{ at } x = x_1(t), \tag{20}$$

$$u + (1 - x_1'(t))H = 0 \text{ at } x = x_1(t), \tag{21}$$

$$H(x, t) = F(x) + h(t) + (x - C)\theta(t). \tag{22}$$

For convenience the superscripts "(1)" of Eqs. (11a) and (11b) have been dropped here and p is written for p_1. The Kutta condition (19) is familiar from the preceding modelling while the underbody-shape relation (22) essentially repeats Eq. (7), although linearized as described above. The conditions (20) and (21) stem from the small-scale Euler region surrounding the moving contact point as expected but with allowance for the free surface development locally.

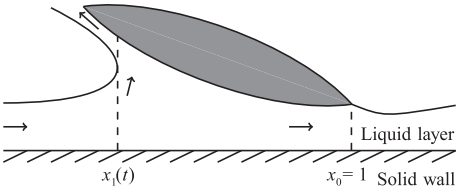

Figure 5 Sketch of a skimming configuration.

3) E. Jolley, and F. T. Smith, Body-air-water interactions and impacts, J. Fluid Mech. in preparation.

Various studies have been performed on the above skimming system. Asymptotic analysis is helpful for small times [2, 18] where the wetted region is initially tiny and for so-called exit time where the body leaves the water and begins its complete rebound into the air. The exit-time analysis [2, 18] is found to be almost identical with that in Eqs. (13a) and (13b). In Fig. 6 a sample solution is shown in which the centre of mass position C is zero. Related interesting properties such as mass and curvature effects or mid-chord impacts of smooth skimming bodies are addressed in Refs. [5, 8, 17-19].

Figure 6a shows progression of the body during the skimming motion as described by three parameters: $Y - Y_0$, the height of the body's centre; $\theta - \theta_0$, the body's rotation; and x_1 the leading-contact position of the water layer along the body (indicating the extent of body wetting by $[x_0, x_1]$). From the x_1 curves, a body's descent ($\mathrm{d}x/\mathrm{d}x < 0$) and ascent ($\mathrm{d}x/\mathrm{d}x > 0$) through the water layer can be seen. While x_1 decreases, the pressure (and thus force) under the body increases. Eventually, this force is sufficient to cause the body to rebound (approximately $t = 2.9$) and ascend back through the water layer to exit (when $x_1 = x_0$).

Throughout this motion, the body's height initially decreases. Although it slightly increases after rebound, it leaves the water at a lower height than it entered due to the deformation of the water. Also, the body rotates in an anti-clockwise manner, decreasing its angle of inclination to the water. Comparing to a flat body (solid lines), a curved body (dashed lines) experiences diminished body wetting (i.e., comparatively larger x_1 values throughout), maintains a slightly lower height after rebound and increased rotation.

Regarding Fig. 6b, the heights of the free-surface under the body and in the wake are shown for a flat body and curved body at different points in the skimming motion. Comparatively, the magnitude of the curved body's wake is slightly reduced at each point in time (range of h values).

Cases of sinking of the body after its impact into water are considered in Ref. [9]. The difference from the previous cases of successful skimming is that the contact point reaches the bodys leading edge $x = -1$ at a finite time, following which a thin layer of water spreads forward along the bodys top surface. This is affected by gravity forces that influence the upper pressure, making p_2 become nonzero. If, in consequence of the forward spread on top, the body eventually sinks then its underbody surface can impact upon the wall (the substrate), again within a finite time. The nature of the impact process on the wall is similar to that considered in Eqs. (13a), (13b), (14a)-(14e) for flat or curved underbodies.

Further work on skimming and sinking is described in a recent paper [3)]: here air effects and fully nonlinear flow are admitted into the modelling.

5. Lift-off, fly-away or bouncing of a body

There are several forms of lift-off which are of interest. The one on which we focus here is that of Ref. [22] as sketched in Fig. 7 and it has a thin body initially at rest on a flat horizontal fixed solid surface or wall given by $y = 0$. The underbody is assumed to be smoothly curved, being convex downwards, and is in touch with the wall at a single contact point $x = C$ which is the position of the centre of mass of the body. So in the fluid-filled gap the initial gap width $H = H_0(x) = F(x) + h_0 + (x - C)\theta_0$ say satisfies

$$H_0 = \frac{\mathrm{d}H_0}{\mathrm{d}x} = 0 \text{ at } x = C \text{ at time } t = 0^-. \tag{23}$$

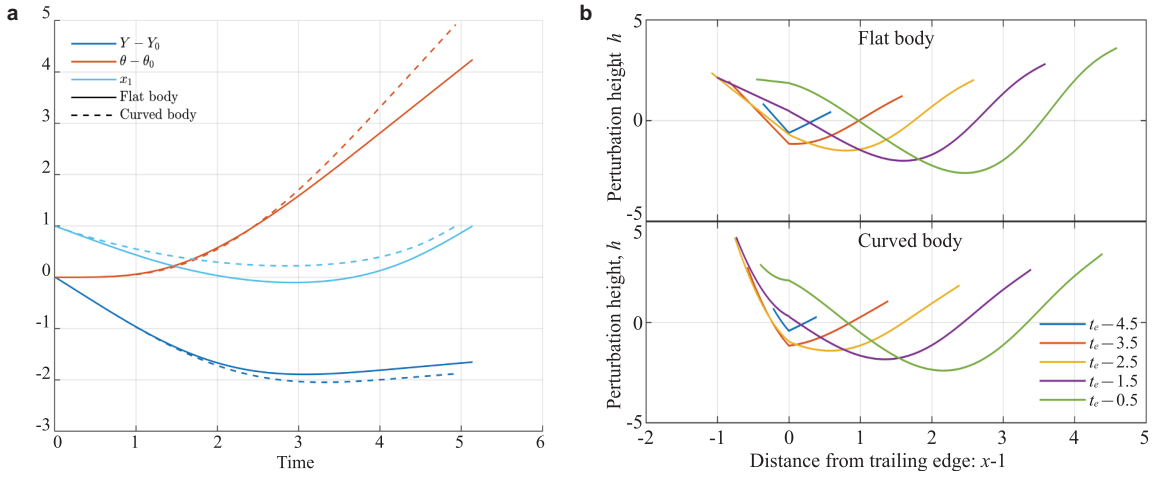

Figure 6 A sample solution showing skimming properties. **a** Comparison of the skimming progression of different body shapes (leading edge position x_1, vertical centre of mass position $Y - Y_0$ and angle of incidence $\theta - \theta_0$). **b** Comparison of the free-surface height under the body and in the wake for different body shapes at several points in time.

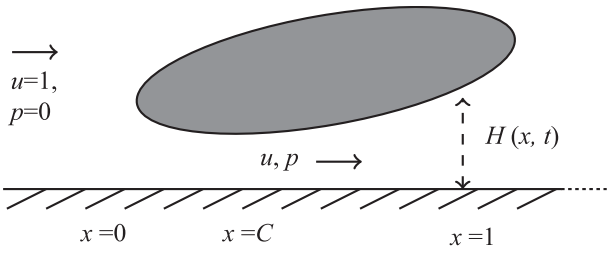

Figure 7 The setup for a body lifting off from a wall.

If the contact point is not at $x = C$ then the body is initially rocking, a case that is considered in Refs. [11, 22] whereas we will address the initially stationary case (23).

Lift-off is induced when the surrounding fluid is set into motion impulsively at time $t = 0^+$ by means of a free oncoming uniform stream $u = 1$ parallel to the wall at atmospheric pressure p of zero. Part of the stream enters the slender gap between the wall and the underbody and thereby creates a pressure force $p(x, t) = p_1(x, t)$ typically of order unity which is sufficient to lift the body off the wall. In contrast, the pressure variation $p_2(x, t)$ on top of the body is only $o(1)$ because of the linearized flow features over the slender body. Given the zero incident vorticity the governing equations in the gap flow are therefore Eqs. (8a) and (8b), derived from Eq. (4) along with the continuity equation, and these are combined with the body-motion equations (5b) and (5c), with p_2 justifiably taken as zero to leading order throughout. The leading and trailing edges of the body have positions $x = 0, 1$ respectively and so the boundary conditions (6c) and (6d) apply at those edges together with a moving-shape relation which is Eq. (22) in essence.

Analysis for small positive times is helpful in checking whether lift-off can indeed occur, or not, and in highlighting the physical scales involved as well as guiding any numerical work on the full problem. It is interesting to examine the details. For most x of $O(1)$, the solution expansion for $0 < t \ll 1$ must take the form:

$$\text{gap width } H(x,t) = H_0(x) + t^2 H_2(x) + \dots, \tag{24a}$$

$$\text{velocity } u(x,t) = t u_1(x) + \dots, \tag{24b}$$

$$\text{pressure } p(x,t) = p_0(x) + \dots, \tag{24c}$$

owing to the balances in the governing equations. Thus Eqs. (8a) and (8b) are in balance at $O(t)$ and $O(1)$ in turn and the $O(1)$ pressure variation then provokes lift and moment contributions of $O(1)$ on the right-hand sides of Eqs. (5b) and (5c), indicating $O(1)$ accelerations of the underbody which are in keeping with the $O(t^2)$ contribution in Eq. (24a). Here the expressions for height $h(t)$ and angle $\theta(t)$ are similar to Eq. (24a). The terms of $O(t^2)$ in the moving gap shape (22), of $O(t)$ in the relation (8a) and of $O(1)$ in the momentum equation (8b) now yield the relations:

$$H_2(x) = h_2 + (x - C)\theta_2, \tag{25a}$$

$$2H_2(x) + (H_0(x)u_1(x))' = 0, \tag{25b}$$

$$u_1(x) = -p_0'(x), \tag{25c}$$

respectively. It follows from Eqs. (25a) and (25c) and from the leading-edge and trailing-edge constraints that the solutions for the velocity perturbation and the pressure at early times are

$$u_1(x) = [-2h_2(x - C) - \theta_2(x - C)^2 + c_1]/H_0(x), \tag{26a}$$

$$p_0(x) = -\int_0^x u_1(s)\,\mathrm{d}s + \frac{1}{2}, \text{ for } 0 < x < C, \tag{26b}$$

$$p_0(x) = -\int_1^x u_1(s)\,\mathrm{d}s, \text{ for } C < x < 1, \tag{26c}$$

effectively in terms of the unknown constants h_2 and θ_2; the constant c_1 is zero for the matching below. A closed problem for h_2 and θ_2 is obtained by virtue of the body movement, giving

$$2Mh_2 = \int_0^1 p_0 \mathrm{d}x - M\hat{g}, \tag{27a}$$

$$2I\theta_2 = \int_0^1 (x - C)p_0 \mathrm{d}x, \tag{27b}$$

from Eqs. (5b) and (5c), with the right-hand sides in Eqs. (27a) and (27b) being linear combinations of h_2 and θ_2 because of Eqs. (26a)-(26c). It can be justified *a posteriori* that the scaled lift and moment are dominated by the outer-solution contributions as in Eqs. (27a) and (27b): the singularity in the velocity (26a) and the corresponding logarithmic responses in the pressure in Eqs. (26b) and (26c) indicate that the above is indeed an outer expansion valid everywhere except very near $x = C$. The inner expansion has

$$(H, u, p) = (O(t^2), O(1), 2h_2\kappa^{-1}\ln(t) + O(1)), \tag{28}$$

where $\xi = (x - C)/t$ is of order unity and the positive constant κ is proportional to the local body curvature. The inner solution smooths out the singularity and logarithmic effect of the outer solution [22] and generates a logarithmically high maximum initial pressure magnitude as indicated in Eq. (28). The criterion for lift-off is examined in detail in Ref. [22] based on the lift response in Eq. (27a).

Large-time analysis is concerned with the possibility of the body flying away to large heights. Here, broadly speaking, the H_t and u_t terms in Eqs. (8a) and (8b) diminish when $t \gg 1$ and hence we find the quasi-steady Bernoulli relation holding for p. Given that, the Mh_{tt} equation then leads to the requirement $M\hat{g} < 1/2$. In more detail, the solution expands in the form:

$$(h, \theta) = t^2(h_2, \theta_2) + \dots, \quad (u, p) = (u_0, p_0) + \dots. \tag{29}$$

So at leading order the gap shape becomes simply $H \sim t^2[h_2 + (x - C)\theta_2]$ whereas the kinematic equation implies that $u_0 = c/[h_2 + (x - C)\theta_2]$ and the momentum balance requires $p_0 = (1 - u_0^2)/2$. Mass multiplied by acceleration then yields the balance:

$$2Mh_2 = \frac{1}{2}\int_0^1 (1 - u_0^2)\mathrm{d}x - M\hat{g}, \tag{30a}$$

and the angular momentum requirement is

$$2I\theta_2 = \frac{1}{2}\int_0^1 (x - C)(1 - u_0^2)\mathrm{d}x. \tag{30b}$$

Combining the above balances gives two nonlinear equations for the unknown constants h_2 and θ_2. The criterion for fly-away stems from the need for h_2 to be positive, giving

$$M\hat{g} < \frac{1}{2}, \tag{31}$$

which follows from Eq. (30a). Comparisons with numerical solutions of the full system and corresponding discussions are presented in Ref. [22]. It is interesting that, unlike the small-time case, the present large-time behaviour shows the influence of the body shape becoming negligible when fly-away occurs.

Features of fly-away in other contexts are described in more recent works. These address the influence of nonzero incident vorticity in both inviscid and viscous scenarios [2)] [20, 21]. An alternative outcome is so-called bouncing [21] as illustrated in Fig. 8, where, repeatedly, the body nearly impacts on the wall but then flies to large heights before once more returning to nearly hit the wall and so on. Repeated excursions into air between skimming events on water are studied in Ref. [5].

6. Viscous effects

Most of the description so far in Sects. 3-5 has been for an assumed inviscid fluid. The assumption of relatively insignificant viscous effects is broadly valid provided no large-scale separation takes place [1, 6, 7].

Significant viscous effects in the area were first studied by Ref. [6] concerning a body within channel flow. The body considered is of length comparable with the channel width and is initially in the so-called core of the flow, thus lying outside the two slender viscous layers near the channel walls. In essence the governing equations (2) and (3) apply now in the core and the wall layers respectively, along with the pressure difference $p_1 - p_2$, and two axial length scales come into operation. Over the $O(1)$ length scale of the body the core is described by the expansion:

$$u = u_0(y) + E_T + Re^{-3/7}u_1(x, y, T) + \ldots, \tag{32}$$

which leads to a linearised version of Eq. (2). Here $u_0(y)$ is typically the parabolic velocity profile of fully developed oncoming flow and time $t = \gamma_1 T$ with γ_1 being large, while E_T denotes passive extra terms produced by matching over a longer length scale. The core flow is combined with the body-motion equations which are essentially Eqs. (5b) and (5c), involving lift and moment as may be expected, but there is an issue of indeterminacy within the $O(1)$ length scale. The indeterminacy arises because the far-field behaviour of the velocity perturbation is found to be given by

$$u_1 \sim (a^{\pm} + b^{\pm}x)u_0'(y) \text{ as } x \text{ tends to } \pm\infty. \tag{33}$$

The constants $a^{\pm}$ and $b^{\pm}$ remain undetermined by the properties over the $O(1)$ length scale. The lift which is found to be proportional to the difference $b^+ - b^-$ is also affected.

The issue is resolved over the longer length scale defined

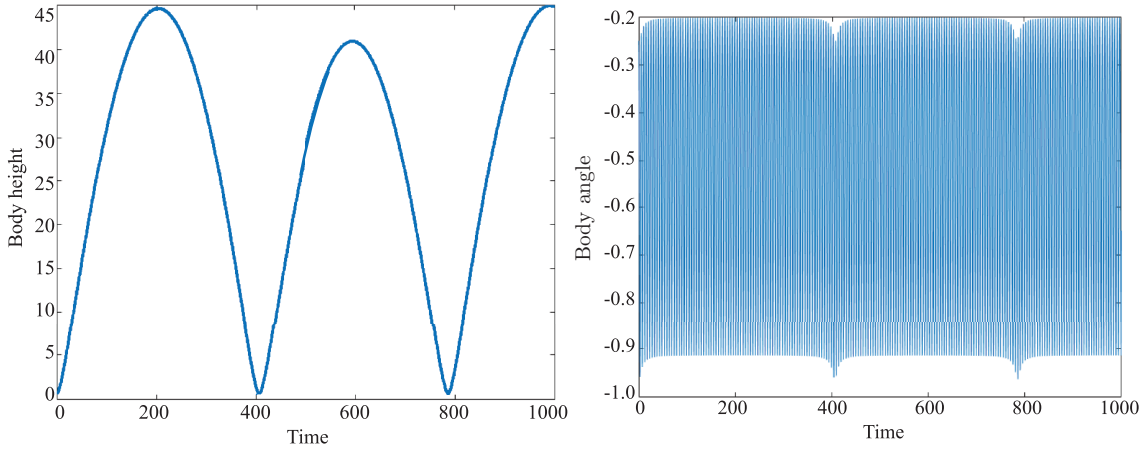

Figure 8 Bouncing indicated by a solution of the system in which quasi-steady flow holds.

by

$$x = Re^{1/7}X, \tag{34}$$

where the core flow solution now has the expansion:

$$u = u_0(y) + O(Re^{-2/7}), \tag{35a}$$
$$p = O(Re^{-4/7}), \tag{35b}$$

while the solutions in the thin viscous-inviscid layers at the lower ($n = 1$) and upper ($n = 2$) channel walls take the form

$$u = Re^{-2/7}U(X, Y, T) + \ldots, \tag{36a}$$
$$p = Re^{-4/7}P_n(X, T) + \ldots, \tag{36b}$$

respectively. Here $y - 1$ or y is scaled with $Re^{-2/7}$ and so Eqs. (36a) and (36b) imply the boundary layer equation (3) holds in effect. The boundary and matching conditions are described in Ref. [6]. A notable effect stems from the relation:

$$P_2 - P_1 \text{ is proportional to } A_{XX}, \tag{37}$$

for the difference between the upper wall pressure and the lower wall pressure, with $A(X, T)$ being the unknown displacement in the core. This relation in tandem with the viscous-inviscid responses in the two wall layers yields upstream influence and downstream influence over the length scale (34) and accounts for the growths (33), which are valid at small values of X, by smoothing them out over the scale (34). A striking result in the linear range is the finding that

$$b^- = -\bar{\mu}b^+. \tag{38}$$

The constant $\bar{\mu} = \cos(\pi/7)$, which is approximately 0.900969, gives the ratio of the streamline slopes for the response (33), over the $O(1)$ length scale of the body. Figure 9 shows the pressures P_1 and P_2 and the displacements D_1 and D_2 induced in the two wall layers of the channel over the longer length scale of Eq. (34); the discontinuities in slopes at the origin over this scale are clear.

A boundary layer setup is addressed in Ref. [7], for which p_2 is zero in effect. The viscous-inviscid boundary layer system is coupled with a displacement which is influenced by the movement of the underbody and hence interacts with Eqs. (5b) and (5c) through the unknown pressure. An additive contribution from the leading edge area is discussed in Ref. [20]. Stabilising properties are also investigated for cases when there is surface flexibility, when the centre of mass is positioned ahead of the midway location or when the body is moving substantially in the streamwise direction.

Viscous-inviscid interplay for a body near a solid surface is studied in Refs. [15,16] with application to boundary layer or channel flow over relatively short streamwise or axial length scales. See also Ref. [14]. These scales are much less than triple-deck lengths for the boundary layer setting and much less than Eq. (34) for the channel setting. The oncoming near-wall flow is a uniform shear flow supplemented by a uniform flow on account of the relative movement of the body upstream or downstream. Jump conditions akin to that in Eq. (6c) are induced. In the overall fluid-body interplay the unknown scaled pressures p_1 and p_2 are comparable; the viscous-inviscid governing equation (3) applies both in the underbody/wall gap and in the region above the overbody and the body moves according to Eqs. (5b) and (5c). An impact at the leading edge is found to occur within a finite time $t = t_0$ in Ref. [16] for the case of a straight plate. Three subregions then form the asymptotic response at $t = t_0^-$ such that nearest the leading edge we have

$$(u, p) = O(1), \quad y = O(t_0 - t), \tag{39}$$

where x is of order $(t_0 - t)^2$, whereas further downstream where x becomes of order $(t_0 - t)$ the expansion is

$$u = O(1), \quad p = O(t_0 - t)^{-1}, \quad y = O(t_0 - t), \tag{40}$$

and the final subregion where x is of order unity exhibits the form

$$(u, p) = O(1), \quad y = O(1). \tag{41}$$

Here Eqs. (39) and (41) leave nonlinear viscous-inviscid effects being important at impact in contrast with Eq. (40) which leads to a linear response. The major contributions to the lift and moment driving the body into the impact are from the subregions where Eqs. (40) and (41) apply. Comparisons with the results of direct simulations of Eq. (1) prove to be affirmative [15, 16]. Other body shapes such as elliptical (see Fig. 10) are investigated in Ref. [**?**] along with the possibility of lift-off emerging via this type of viscous-inviscid interplay.

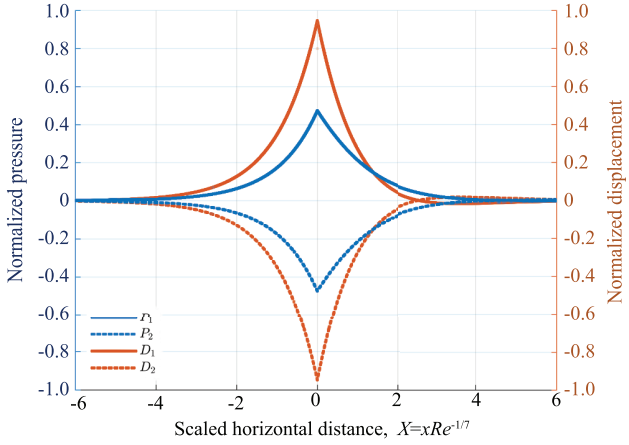

Figure 9 Long-scale pressure and displacement in the channel wall layers for the viscous-inviscid situation of Eqs. (32)-(38).

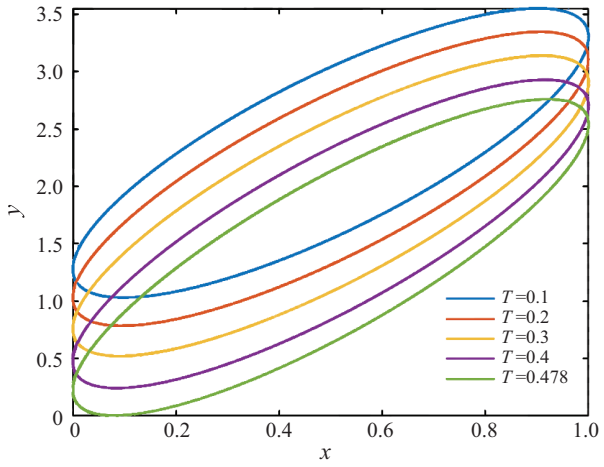

Figure 10 A solution of the viscous-inviscid case in near-wall flow for an elliptical body.

7. Further discussion and conclusion

Progress in understanding dynamic fluid/body interactions and the range of mechanisms at play has been reviewed in this article for the case of a single body involved in an unsteady two-dimensional interaction. We have considered the fundamental modelling together with interactions and impacts in inviscid flows, skimming and sinking, the lift-off, fly-away or bouncing of a body, while viscous effects studied have included the feedback between viscous and inviscid contributions. Another viscous effect which is notable in passing occurs when a water droplet approaches a wall, leading to a different form of viscous/inviscid feedback between quasi-inviscid water and viscous air motion in the phenomenon of air cushioning, a phenomenon which has attracted much analytical and simulation attention recently. The present work on fluid-body interactions has highlighted physical and mechanical insights in particular into impact times, lift-off criteria, the evolution towards impact or towards fly-away, the influences from body shape and mass for example and the influence of the main parameters.

Other ongoing or recent works are also of interest. Our attention has mostly been on analytical developments and especially on interactions in the presence of relatively thin or slender bodies with near-aligned surrounding fluid flow. Studies of non-slender bodies are in recent work for inviscid-fluid interactions; thus Ref. [10] addresses the scenario of several circular bodies moving freely in an otherwise uniform stream, and Ref. [33] discusses the free movements of an ellipse with aspect ratio of order unity. Inviscid fluid-body interaction is described within a channel which has significantly non-parallel walls [1)], while in Ref. [34] the basics of fluid-body interaction for a long near-wall body in channel flow are addressed with active viscous-inviscid interplay being present. It seems obvious that there are many gaps to be filled yet in terms of understanding mechanisms and their application.

Certain clear challenges for the future are as follows. The extension of understanding to many bodies in surrounding flowing fluid would be of considerable value. This has been begun in Refs. [10, 32]. Likewise extending the theory rationally to allow for rebounds would be desirable; a start is being made [1)]. There is also a call for increased allowance for flow separation, whether inviscid or viscous, during fluid-body evolutions. Dynamic interactions involving time and three spatial dimensions [23] are still in their infancy as regards physical understanding and modelling. This list of challenges is not an exhaustive one but is meant to indicate potential areas of interest.

Author contributions *Frank T Smith contributed to conceptualization, formal analysis, funding acquisition, methodology, supervision, validation, writing original draft, and writing review & editing. Ryan A Palmer and Ellen M Jolley contributed to formal analysis, methodology, validation, visualization, writing original draft, and writing review & editing.*

Acknowledgements *We acknowledge gratefully helpful discussions with colleagues Andrew Ellis, Samire Yazar, Qingsong Liu, T D Dang, Phil Wilson, Kevin Liu, Ted Johnson, Robert Bowles, Sergei Timoshin and with staff at Aerotex UK, namely Colin Hatch, Ian Roberts, Richard Moser and Roger Gent. Support from the Engineering and Physical Sciences Research Council (Grants Nos. EP/R511638/1, GR/T11364/01, EP/G501831/1, EP/H501665/1, and EP/K032208/1), University College London (two IAA awards) and Aerotex UK is also acknowledged with gratitude. Thanks are due to the Beijing International Center for Theoretical and Applied Mechanics for their interest and invitation concerning this article.*

1 F. T. Smith, and A. S. Ellis, On interaction between falling bodies and the surrounding fluid, Mathematika **56**, 140 (2010).
2 P. D. Hicks, and F. T. Smith, Skimming impacts and rebounds on shallow liquid layers, Proc. R. Soc. A **467**, 653 (2011).
3 F. T. Smith, and P. L. Wilson, Fluid-body interactions: clashing, skimming, bouncing, Phil. Trans. R. Soc. A **369**, 3007 (2011).
4 F. T. Smith, and P. L. Wilson, Body-rock or lift-off in flow, J. Fluid Mech. **735**, 91 (2013), arXiv: 1301.2365.
5 K. Liu, and F. T. Smith, Collisions, rebounds and skimming, Phil. Trans. R. Soc. A **372**, 20130351 (2014).
6 F. T. Smith, and E. R. Johnson, Movement of a finite body in channel flow, Proc. R. Soc. A **472**, 20160164 (2016).
7 F. T. Smith, Free motion of a body in a boundary layer or channel flow, J. Fluid Mech. **813**, 279 (2017).

8 K. Liu, and F. T. Smith, A smoothly curved body skimming on shallow water, J. Eng. Math. **128**, 17 (2021).
9 F. T. Smith, and K. Liu, Flooding and sinking of an originally skimming body, J. Eng. Math. **107**, 37 (2017).
10 F. Smith, S. Balta, K. Liu, and E. R. Johnson, On dynamic interactions between body motion and fluid motion, in: Mathematics Applied to Engineering, Modelling, and Social Issues (Springer, Cham, 2019), pp. 45-89.
11 S. Balta, On fluid-body and fluid-network interactions, Dissertation for Doctoral Degree (University College London, London, 2017).
12 R. A. Palmer, I. Roberts, C. Hatch, R. Moser, and F. Smith, Non-spherical particle trajectory modelling for ice crystal conditions, SAE Technical Paper, 2019.
13 F. Smith, and R. Palmer, A freely moving body in a boundary layer: Nonlinear separated-flow effects, Appl. Ocean Res. **85**, 107 (2019).
14 R. A. Palmer, and F. T. Smith, When a small thin two-dimensional body enters a viscous wall layer, Eur. J. Appl. Math. **31**, 1002 (2020).
15 R. A. Palmer, and F. T. Smith, A body in nonlinear near-wall shear flow: Numerical results for a flat plate, J. Fluid Mech. **915**, A35 (2021).
16 R. A. Palmer, and F. T. Smith, A body in nonlinear near-wall shear flow: Impacts, analysis and comparisons, J. Fluid Mech. **904**, A32 (2020).
17 R. A. Palmer, and F. T. Smith, Skimming impacts and rebounds of smoothly shaped bodies on shallow liquid layers, J. Eng. Math. **124**, 41 (2020).
18 R. A. Palmer, and F. T. Smith, Skimming impact of a thin heavy body on a shallow liquid layer, J. Fluid Mech. **940**, A6 (2022).
19 R. A. Palmer, and F. T. Smith, The role of body shape and mass in skimming on water, Proc. R. Soc. A. **479**, 20220311 (2023).
20 E. M. Jolley, R. A. Palmer, and F. T. Smith, Particle movement in a boundary layer, J. Eng. Math. **128**, 6 (2021).
21 E. M. Jolley, and F. T. Smith, A heavy body translating in a boundary layer: 'Crash', 'fly away' and 'bouncing' responses, J. Fluid Mech. **936**, A37 (2022).
22 S. Balta, and F. T. Smith, Fluid flow lifting a body from a solid surface, Proc. R. Soc. A **474**, 20180286 (2018).
23 F. T. Smith, and K. Liu, Three-dimensional evolution of body and fluid motion near a wall, Theor. Comput. Fluid Dyn. **36**, 969 (2022).
24 G. Hall, On the mechanics of transition produced by particles passing through an initially laminar boundary layer and the estimated effect on the lfc performance of the x-21 aircraft, Technical Report (NASA, 1964).
25 S. Einav, and S. L. Lee, Particles migration in laminar boundary layer flow, Int. J. Multiphase Flow **1**, 73 (1973).
26 H. Petrie, Morris, A. Bajwa, and D. Vincent, Transition induced by fixed and freely convecting spherical particles in laminar boundary layers, Technical Report (Pennsylvania State Univ University Park Applied Research Lab, 1993).
27 J. Wang, and E. K. Levy, Particle behavior in the turbulent boundary layer of a dilute gas-particle flow past a flat plate, Exp. Thermal Fluid Sci. **30**, 473 (2006).
28 C. Schmidt, and T. Young, in Impact of freely suspended particles on laminar boundary layers: Proceedings of 47th AIAA Aerospace Sciences Meeting including The New Horizons Forum and Aerospace Exposition, Orlando, 2009.
29 M. Dehghan, and H. Basirat Tabrizi, Effects of coupling on turbulent gas-particle boundary layer flows at borderline volume fractions using kinetic theory, J. Heat Mass Transf. Res. **1**, 1 (2014).
30 L. M. Portela, P. Cota, and R. V. A. Oliemans, Numerical study of the near-wall behaviour of particles in turbulent pipe flows, Powder Tech. **125**, 149 (2002).
31 V. Loisel, M. Abbas, O. Masbernat, and E. Climent, The effect of neutrally buoyant finite-size particles on channel flows in the laminar-turbulent transition regime, Phys. Fluids **25**, 123304 (2013).
32 Q. Liu, S. Yazar, and F. Smith, On interaction between freely moving bodies and fluid in a channel flow, Theor. Appl. Mech. Lett. **13**, 100413 (2023).
33 D. W. K. Sin, Fluid-Body Interactions, Dissertation for Doctoral Degree (University College London, London, 2017).
34 F. T. Smith, and P. Servini, Channel Flow Past A Near-Wall Body, Q. J. Mech. Appl. Math. **72**, 359 (2019).

流体 - 固体相互作用、碰撞和起飞的建模

Frank T Smith, Ellen M Jolley, Ryan A Palmer

摘要 本文是流体 - 固体相互作用机制方面的最新进展综述, 主要研究固体物体自身的运动与其周围流体运动之间的相互影响. 非稳态相互作用的数学模型是对两个空间维度和时间尺度的内部通道和外部近壁流的描述. 本文重点描述伴随计算量减少的分析发展过程. 文章讨论无黏性流中掠过和下沉、物体的起飞、飞离或弹跳, 以及黏性效应, 特别是黏性和无黏性之间的相互作用和影响. 主要研究结果涉及撞击时间、起飞条件、撞击和飞离之间的边界、主要参数及其范围以及物体形状和质量对物理及力学机制的影响.